Proc. Natl. Acad. Sci. USA
Vol. 95, pp. 15049–15054, December 1998
Neurobiology

Elevated anxiety and antidepressant-like responses in serotonin 5-HT_{1A} receptor mutant mice

LORA K. HEISLER*†, HUNG-MING CHU*†, THOMAS J. BRENNAN*‡, JEAN A. DANAO*, PREETPAUL BAJWA*, LOREN H. PARSONS§, AND LAURENCE H. TECOTT*‖

*Department of Psychiatry and Center for Neurobiology and Psychiatry, University of California, San Francisco, 401 Parnassus Avenue, San Francisco, CA 94143-0984; and §The Scripps Research Institute, 10550 North Torrey Pines Road, La Jolla, CA 92037

Edited by Stanley B. Prusiner, University of California, San Francisco, CA, and approved October 7, 1998 (received for review September 1, 1998)

ABSTRACT **The brain serotonin (5-hydroxytryptamine; 5-HT) system is a powerful modulator of emotional processes and a target of medications used in the treatment of psychiatric disorders. To evaluate the contribution of serotonin 5-HT_{1A} receptors to the regulation of these processes, we have used gene-targeting technology to generate 5-HT_{1A} receptor-mutant mice. These animals lack functional 5-HT_{1A} receptors as indicated by receptor autoradiography and by resistance to the hypothermic effects of the 5-HT_{1A} receptor agonist 8-hydroxy-2-(di-*n*-propylamino)tetralin (8-OH-DPAT). Homozygous mutants display a consistent pattern of responses indicative of elevated anxiety levels in open-field, elevated-zero maze, and novel-object assays. Moreover, they exhibit antidepressant-like responses in a tail-suspension assay. These results indicate that the targeted disruption of the 5-HT_{1A} receptor gene leads to heritable perturbations in the serotonergic regulation of emotional state. 5-HT_{1A} receptor-null mutant mice have potential as a model for investigating mechanisms through which serotonergic systems modulate affective state and mediate the actions of psychiatric drugs.**

The brain serotonin (5-hydroxytryptamine; 5-HT) system has been strongly implicated in the neural regulation of mood and anxiety state. Accordingly, many commonly used antidepressant and antianxiety medications target this system (1). The complex physiological actions of serotonin are mediated by a heterogeneous family of at least 14 distinct receptor subtypes (2). Although the relative contributions of individual receptor subtypes to the serotonergic regulation of mood are incompletely understood, particular attention has focused on the 5-HT_{1A} receptor subtype. Partial agonists at this receptor, such as buspirone, are in clinical use as anxiolytics (3), and 5-HT_{1A} receptor antagonists are reported to accelerate the therapeutic effects of antidepressant medications (4).

These compounds produce complex effects on brain function through interactions with functionally distinct populations of 5-HT_{1A} receptors. 5-HT_{1A} receptors located on serotonergic neuronal cell bodies and dendrites are the predominant somatodendritic autoreceptors of these neurons; their activation suppresses serotonergic neuronal activity (5, 6). In addition, postsynaptic 5-HT_{1A} receptors are expressed in numerous serotonergic projection sites such as the cerebral cortex, septal nuclei, hippocampus, and amygdala (7). The relatively selective 5-HT_{1A} receptor agonist 8-hydroxy-2-(di-*n*-propylamino) tetralin (8-OH-DPAT) and antagonist WAY 100635 (8) have been used as pharmacological probes of 5-HT_{1A} receptor function. Systemic administration of 8-OH-DPAT produces hyperphagia, hypothermia, and an anxiolytic-like effect in rodents (9–12). The behavioral and physiological effects of 8-OH-DPAT are blocked by pretreatment with WAY 100635 (12–14).

To complement pharmacological approaches to the study of 5-HT_{1A} receptor function, we have used a gene-targeting strategy to generate a line of mice bearing a complete and specific elimination of this receptor subtype. We report that these animals display a pattern of behavioral changes that sheds light on the functional roles of the 5-HT_{1A} receptor subtype in neural pathways relevant to anxiety and depression.

MATERIALS AND METHODS

Targeting Vector. An 80- to 100-kb genomic fragment was isolated from a 129/Sv genomic P1 library (Genome Systems, St. Louis) by using PCR primers generated to sequences within the intronless 5-HT_{1A} receptor gene protein-coding region. Gene fragments were subcloned into a pBluescript II SK (Stratagene) vector for further manipulation. A 1.5-kb *Pst*I genomic fragment, including a portion of protein-coding region, was replaced by a neomycin resistance cassette under the regulation of a phosphoglycerate kinase promoter (Fig. 1*A*). This mutation was designed to produce a loss of function by truncating the 5-HT_{1A} receptor protein at the third cytoplasmic loop. The neomycin resistance cassette was flanked by 1.7 kb of homologous genomic sequence at its 5′ aspect and by 6.9 kb of homologous genomic sequence at its 3′ aspect. The mutated fragment was cloned into a phosphoglycerate kinase–thymidine kinase plasmid (PGK-TK) containing the herpes simplex virus thymidine kinase gene driven by the phosphoglycerate kinase promoter in a Bluescript SK vector.

Generation of Homologous Recombinant Clones. 129/SvJ-derived JM1 embryonic stem (ES) cells (15) were electroporated with linearized targeting vector, and drug selection was applied in a positive/negative selection strategy (16) to enrich for targeted clones. Surviving ES cell colonies were screened for homologous recombination by using Southern blot analysis. A genomic fragment corresponding to a region 5′ to the expected integration site was used to probe genomic DNA digested with *Bam*HI. Wild-type and mutant alleles were indicated by 12.3-kb and 6.5-kb fragments, respectively (Fig. 1).

Generation of 5-HT_{1A} Receptor-Null Mutant Mice. Male chimeras produced by injection of targeted ES cells into C57BL/6J blastocysts were bred with C57BL/6J females. Germ-line transmission of the targeted mutation was verified by Southern blot analysis of tail DNA. Heterozygotes were then mated with C57BL/6J mice, and the resulting heterozygous animals were crossed, producing homozygous mutant,

The publication costs of this article were defrayed in part by page charge payment. This article must therefore be hereby marked "*advertisement*" in accordance with 18 U.S.C. §1734 solely to indicate this fact.

This paper was submitted directly (Track II) to the *Proceedings* office.
Abbreviations: 8-OH-DPAT, 8-hydroxy-2-(di-*n*-propylamino)tetralin; 5-HT, 5-hydroxytryptamine; ES, embryonic stem.
†L.K.H. and H.-M.C. contributed equally to this work.
‡Present address: Deltagen, 1031 Bing Street, San Carlos, CA 94070.
‖To whom reprint requests should be addressed. e-mail: tecott@itsa.ucsf.edu.

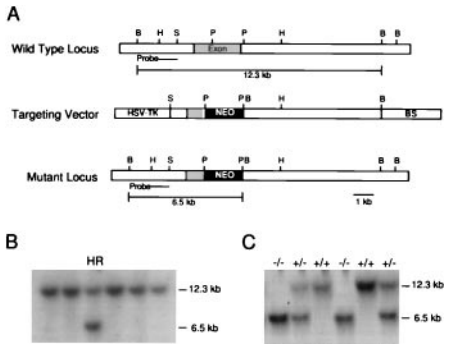

FIG. 1. (*A*) A schematic representation of the 5-HT_{1A} receptor gene, targeting construct, and the mutant allele. The region corresponding to the probe used for Southern blotting is indicated. (*B*) A representative Southern blot of *Bam*HI-digested ES cell genomic DNA; the wild-type allele is indicated by a 12.3-kb band and the homologous recombinant (HR) allele indicated by a 6.5-kb band. (*C*) Southern blot of mouse tail genomic DNA from wild type (+/+), heterozygous (+/−), and homozygous mutant (−/−) animals. HSV-TK, herpes simplex virus thymidine kinase gene; BS, pBluescript SK vector; NEO, neomycin resistance cassette; B, *Bam*HI; H, *Hin*dIII; S, *Sal*I; P, *Pst*I.

heterozygous, and wild-type mice. Animals of this generation were used for the studies reported. Mice were group-housed 2–6 mice per cage with free access to food and water under a 12-hr light/dark cycle (lights on at 0600 hr). For behavioral and physiological experiments, investigators were blind to animal genotype.

Northern Blot Analysis. Northern blot analysis was performed by using 20 μg of whole-brain total RNA extracted with the guanidinium isothiocyanate/phenol procedure (17). A 1.5-kb genomic fragment corresponding to the region deleted from the targeting vector was ^{32}P-radiolabeled by random prime labeling. After hybridization, washes, and film development, blots were stripped and rehybridized with a cyclophilin probe (internal standard).

Immunohistochemistry. Mice were perfused pericardially with PBS followed by a 4% paraformaldehyde solution. Brains were post-fixed in the same fixative, cryoprotected in sucrose solutions (in PBS), frozen in powdered dry ice, and stored in −70°C until use. Cryostat (40-μm) sections from comparable levels of wild-type and mutant brains were selected and processed in parallel. Sections were incubated for 1 hr at room temperature in a blocking solution followed by incubation with the primary antibody for 2 days at 4°C. Primary antibodies and their dilutions were rabbit anti-serotonin (Incstar, Stillwater, MN; 1:15,000 dilution), rabbit anti-serotonin transporter (Incstar, 1:12,500 dilution), rabbit anti-tyrosine hydroxylase (Pel-Freez Biologicals; 1:5,000 dilution). A biotinylated goat anti-rabbit secondary antibody (Vector Laboratories; 1:200 dilution) was applied for 30 min, followed by a 30-min incubation in avidin-biotin horseradish peroxidase complex (Vector Laboratories). Peroxidase label was detected by incubation in 3,3′-4,4′-diaminobenzidine (DAB; Sigma).

Receptor Autoradiography. Fresh frozen brains were cut into 20-μm sections and stored at −20°C until use. Immediately after thawing, sections were incubated for 15 min in incubation buffer (0.17 M Tris·HCl, pH 7.7/4 mM $CaCl_2$/0.01% ascorbic acid/10 μM pargyline). To assess nonspecific binding, one of each pair of adjacent sections was incubated for another 10 min in incubation buffer with 10 μM serotonin. Sections were then incubated with 2 nM [^{3}H]8-OH-DPAT (NEN) for 45 min, followed by two 5-min washes in ice-cold incubation buffer. Sections were then dried with a stream of cool air, apposed to Hyperfilm-^{3}H (Amersham), and developed with D-19 solution (Kodak) after a 2-wk exposure.

Tissue Monoamine Determinations. After decapitation, dissection of the medial prefrontal cortex, hippocampus, and hypothalamus were rapidly performed, and tissue samples were frozen and stored at −70°C until analysis. Monoamines and their metabolites were extracted from tissue homogenates by using perchloric acid and then quantified from 100-μl volumes of the supernatant injected onto an HPLC system: 4 × 300 mm column; 5 μM Resolve C_{18} stationary phase (Waters); mobile phase of 166 mM citric acid, 25 mM sodium acetate, 0.1 mM Na_2·EDTA, 1.2 mM sodium octyl sulfate, 28.9 mM triethylamine, and 10% MeOH (vol/vol; apparent pH 2.5). The flow rate was 0.5 ml/min. Analytes were detected electrochemically, and monoamine concentrations were estimated by using external calibration curves that were generated daily.

Behavioral Testing. Behavioral assays were performed in mice between the ages of 10 and 14 weeks. Approximately 3 min before each assay, animals were removed from their home cage and placed in a clean holding cage, unless otherwise specified. Between subjects, instruments were cleaned with a 0.25% bleach solution, wiped down with water, and then dried. All standard polycarbonate mouse (29 × 18.5 × 13 cm) and rat (48 × 27 × 13 cm) cages used during testing were autoclaved between subjects. Subjects were divided into two groups; one group was assessed in the home-cage activity, open-field, and elevated-zero maze tests (n = 10 per genotype), whereas the other was examined in the rotorod, tail-suspension, and thermoregulation assays (n = 9 per genotype). All subjects were included in the novel-object assay. Unless otherwise noted, all animals were tested in a particular behavioral assay on the same day during the light cycle. All experimental conditions were counterbalanced by genotype.

Home-Cage Activity. Animals were housed individually in rat cages with bedding, food, and water. To assess activity, beam breaks were collected each hr for 72 hr with a photobeam activity system (San Diego Instruments). Both horizontal locomotor activity (4 × 8 array of infrared photobeams) and rearings (elevated set of eight infrared photobeams) were monitored. The first 24 hr were considered an acclimation period, and the subsequent 48 hr of activity were analyzed.

Rotorod. Motor coordination was assessed with an Accurotor rotorod (Accuscan Instruments, Columbus, OH) set at an acceleration rate of 2 rpm per 15 sec. Four animals were tested concurrently in separated 11-cm-wide compartments on a rod approximately 3 cm in diameter and elevated 35 cm. Each animal was assessed 3 times with a 1-hr intertrial interval. Performances in trials 1–3 were averaged for data analysis.

Open Field. A 4-unit open field was used, consisting of a white Kydex box divided into 4 separate 50 × 50 × 38 cm chambers, allowing 4 animals to be tested concurrently. A video camera was mounted directly above the chambers. Each chamber was divided into peripheral (within 7 cm of the chamber walls) and central (area within the periphery) regions. Distance traveled, time spent in the central vs. peripheral areas of the field, and number of entrances into the central area were assessed for 30 min with a video tracking system (Poly-Track, San Diego Instruments).

Elevated Zero Maze. This maze is an elevated (42 cm), white, annular (46-cm diameter) runway (5.5-cm width) divided into 4 quadrants; 2 opposing "open" quadrants without walls (3-mm lip) and 2 opposing "closed" quadrants (11-cm high walls). A video camera was mounted directly above the maze. Mice were placed in the closed quadrant of the maze, and activity was collected for 5 min. Time spent in the open quadrants was monitored with a stopwatch. Numbers of open-quadrant entrances, head dips, stretch-attend postures, rearing, and fecal boli were also recorded. Total activity and activity in the open quadrants of the maze were recorded automatically by using the video tracking system. Animals received 2 test sessions, 2 weeks apart.

Novel Object. Approximately 16 hr before novel-object exposure, animals were housed individually in rat cages with bedding, food, and water, and activity was collected with the photobeam system. During the light cycle (1030–1230 hr), a novel object (white table tennis ball, Harvard, 2-Star) was taped to the corner of the cage farthest from the nest, and activity was monitored for the next 30 min. Beam breaks were collected to record activity and time and entrances into the area where the novel object was located (defined as a 175-cm^2 region bounded by the corner of the cage). Latency to enter this region was scored with a stopwatch. Time spent in the nest area while the novel object was in the cage was also determined (also defined as a 175-cm^2 region).

Tail Suspension. Mice were suspended by the tail from a metal bar (1.2-cm diameter) elevated 30 cm in a visually isolated area. Behavior was videotaped for 6 min. Immobilization time during tail suspension was scored with a stopwatch from the videotape. Animals were tested in 2 groups on consecutive days.

8-OH-DPAT-Induced Hypothermia. Mice were transferred to holding cages 30 min before drug administration. (+)-8-OH-DPAT (Research Biochemicals, Natick, MA) was dissolved in 0.9% saline and injected subcutaneously (0, 0.05, 0.2, and 1.0 mg/kg). A thermistor probe was inserted 1.5 cm into the rectum, and the temperature reading was recorded (TH-5 thermometer; Physitemp, Clifton, NJ) 20 and 10 min before and 10, 20, 30, 40, 50, and 60 min after drug treatment. Each animal received all doses in a counterbalanced manner, with a 4-day latency period between treatments.

Statistics. All behavioral scores were analyzed for normality by using the Shapiro-Wilk's W test. One-way ANOVA or repeated-measures ANOVA followed by Tukey HSD post hoc tests were used to compare the effect of genotype on normally distributed variables. Genotype comparisons of variables that were not normally distributed were analyzed with the Kruskal–Wallis H test followed by Tukey HSD post hoc tests. All figures display the mean ± SE of the data to illustrate the central tendency of the variables. For all analyses, significance was assigned at the $P \leq 0.05$ level.

RESULTS

Homologous recombinant ES cell clones were produced with an overall frequency of approximately 1/100 drug-resistant colonies (Fig. 1*B*). Blastocyst injections of targeted cells resulted in chimeric mice that were bred with C57BL/6J females. Germ-line transmission of the mutation was confirmed by Southern blot analysis (Fig. 1*C*). Heterozygote crossing produced wild-type, heterozygous, and homozygous mutant mice in the expected Mendelian ratios, indicating that the mutation does not impair embryonic viability. 5-HT_{1A} receptor mutant mice were healthy and normal in appearance.

To assess the abundance of intact 5-HT_{1A} receptor mRNA within the brains of mutant mice, Northern blot analysis was performed. The blot was probed with a radiolabeled fragment corresponding to the deleted region of the gene. A ≈5.5-kb band was apparent in the wild-type, but not the mutant, lane (Fig. 2*A*). A ≈50% reduction in the abundance of intact transcript was observed in heterozygous animals. To detect 5-HT_{1A} receptor-binding sites, receptor autoradiography was performed using [^{3}H]8-OH-DPAT (Fig. 2*B*). In wild-type sections, the distribution of binding conformed to prior reports (7), and no specific autoradiographic signal was observed in brain sections from homozygous mutant mice. Heterozygous sections exhibited an intermediate level of binding.

No differences were observed in brain weights of wild-type, heterozygous, or homozygous mutant mice. Evaluation of Nissl-stained sections throughout the neuraxis revealed no apparent cytoarchitectural abnormalities. Serotonin immunocytochemistry revealed no overt abnormalities in the distribution of serotonergic neurons (Fig. 3) in homozygous mutant mice. Similarly, serotonin transporter immunocytochemistry revealed no apparent differences in the distribution or density of serotonergic fiber staining. For example, the distribution of serotonergic fibers within the hippocampal formation appeared normal in mutant brains, with the characteristic dense innervation of the lacunosum moleculare layer of Ammon's horn (Fig. 3). Because of known interactions between serotonin and catecholaminergic neural systems, the distribution of catecholaminergic neurons was assessed by using tyrosine hydroxylase immunocytochemistry; no phenotypic differences were noted (Fig. 3). Levels of serotonin, dopamine, and their metabolites were also determined in mutant mice. HPLC analysis of extracts from the prefrontal cortex, hippocampus, and hypothalamus revealed no abnormalities (data not shown).

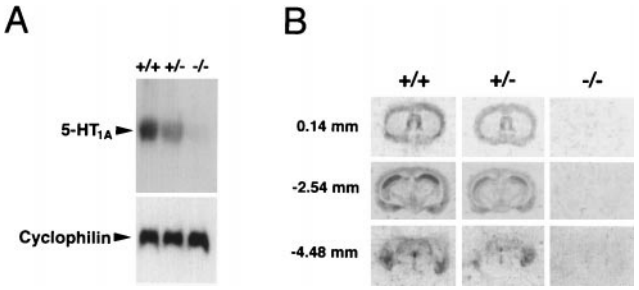

FIG. 2. (*A*) Northern blot analysis of 5-HT_{1A} receptor gene expression in wild-type (+/+), heterozygous (+/−), and homozygous mutant (−/−) animals. A cyclophilin probe demonstrated equivalent RNA loading in all lanes. (*B*) [^{3}H]8-OH-DPAT autoradiography of representative sections at the level of the septal nuclei (*Top*), midhippocampal formation (*Middle*), and dorsal raphe nucleus (*Bottom*). Anterior/posterior coordinates in mm relative to bregma are indicated, in accordance with the mouse-brain atlas of Franklin and Paxinos (39).

Diurnal patterns of activity were monitored for animals individually housed in photobeam enclosures. A repeated-measures ANOVA revealed a significant main effect of time on activity, such that animals were more active in the dark

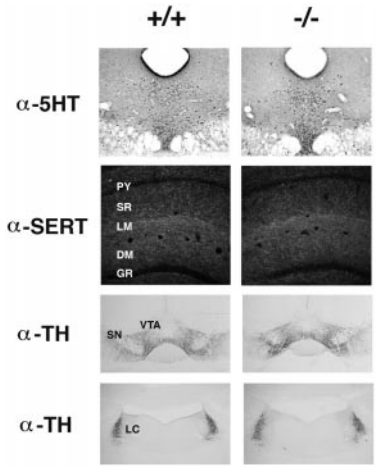

FIG. 3. Immunohistochemical analysis of monoaminergic neurons in wild-type (+/+) and homozygous mutant (−/−) brains. Dorsal raphe serotonin neurons labeled with an anti-serotonin antibody (α-5-HT). Darkfield view of serotonergic innervation of the dorsal hippocampus labeled with an anti-serotonin transporter antibody (α-SERT). Dopaminergic neurons of the substantia nigra (SN) and ventral tegmental area (VTA) labeled with an anti-tyrosine hydroxylase antibody (α-TH). Noradrenergic neurons of the locus coeruleus (LC) labeled with α-TH. PY, CA1 pyramidal layer; SR, striata radiatum; LM, lacunosum moleculare; DM, dentate gyrus molecular layer; GR, dentate gyrus granule-cell layer.

phase than in the light phase ($F_{1,29} = 30.21$, $P \leq 0.01$). However, no phenotypic differences in activity levels or diurnal activity patterns were observed [48-hr total distance (cm) during light cycle: +/+, 10,933 ± 830, +/−, 15,220 ± 2,525, −/− 13,170 ± 2,428; dark cycle: +/+, 47,733 ± 6,370, +/−, 39,173 ± 6,095, −/−, 36,058 ± 3,518]. Similarly, one-way ANOVA revealed no differences by genotype in motor coordination on the accelerating rotorod assay.

Analysis of open-field behavior revealed a significant effect of genotype on time spent ($F_{2,25} = 6.65$, $P \leq 0.01$), distance traveled ($F_{2,25} = 10.20$, $P \leq 0.01$), and entrances into the central area of the enclosure ($F_{2,25} = 12.09$, $P \leq 0.001$; Fig. 4). Post hoc comparisons indicated that wild-type mice spent more time, were more active, and entered the center of the open field more frequently than did mutant and heterozygous animals. No differences in total activity in the open field by genotype were observed.

Significant phenotypic effects were found in open-quadrant behavior in the elevated-zero maze. As these effects did not differ between trials 1 and 2, data were collapsed for analysis (Fig. 5). A significant genotype effect was found on time spent ($F_{2,26} = 9.28$, $P \leq 0.01$) and distance traveled (Kruskal–Wallis $H_2 = 6.17$, $P \leq 0.05$) in the open quadrants (Fig. 5 *A* and *B*). Post hoc comparisons indicated that open-quadrant time and activity were reduced in mutant mice relative to wild-type animals. Mutants also displayed less time in the open quadrants than did heterozygotes. ANOVA revealed a trend toward a phenotype effect in open-quadrant entrances; direct comparisons of mutant and wild-type groups revealed a significant difference ($t_{17} = 2.44$, $P \leq 0.05$; Fig. 5*C*), indicating that mutants were less likely to enter the open quadrants. A significant effect was also observed in the frequency of head dips displayed by genotype ($F_{2,28} = 4.35$, $P \leq 0.05$; Fig. 5*D*), with heterozygous animals exhibiting a greater number than mutant mice. No differences in total activity or frequency of stretch-attend postures, fecal boli, or rearing were observed by genotype on the elevated-zero maze.

Marked differences also were found in the response of mutant and wild-type animals to the presentation of a novel object. A significant genotype effect was observed in the latency to approach the object ($H_2 = 9.95$, $P \leq 0.01$; Fig. 6*A*), with homozygous mutants exhibiting significantly greater latencies than heterozygous or wild-type mice. Significant phenotypic differences also were found in the number of entries

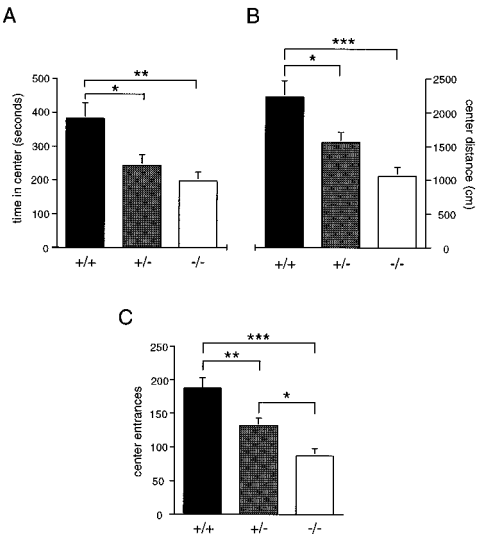

FIG. 4. Locomotor behavior in the open field. Mean (±SEM) time (*A*), distance (*B*), and entrances (*C*) into the central region of an open field during a 30-min exposure. Significant differences by genotype are indicated as ***, $P \leq 0.001$; **, $P \leq 0.01$; *, $P \leq 0.05$.

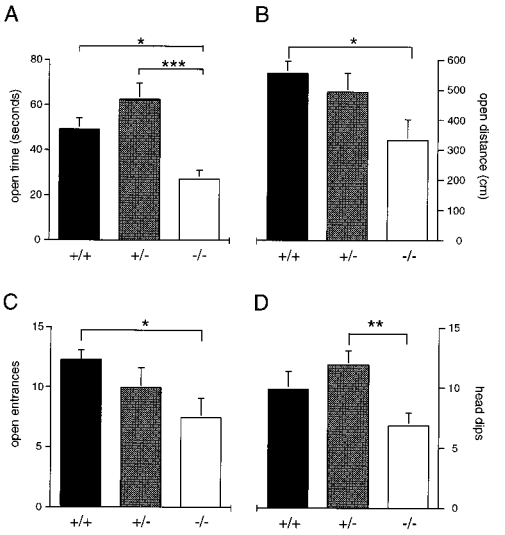

FIG. 5. Behavior in the elevated-zero maze. Mean (±SEM) time (*A*), distance (*B*), open-quadrant entrances (*C*) and head dips (*D*) in the open quadrants of an elevated-zero maze during a 5-min trial. Significant differences by genotype are indicated as ***, $P \leq 0.001$; **, $P \leq 0.01$; *, $P \leq 0.05$.

into the region of the novel object ($H_2 = 7.40$, $P \leq 0.05$; Fig. 6*B*) and time spent in the nest area ($H_2 = 6.93$, $P \leq 0.05$) during the 30-min test session. Post hoc analysis indicated that mutant mice were less likely to approach the novel object and more likely to spend time in their nest than wild-type mice. Although no differences in overall activity by genotype were evident before novel-object presentation, a significant genotype effect was observed in horizontal ($H_2 = 9.22$, $P \leq 0.01$) and vertical ($H_2 = 10.83$, $P \leq 0.01$) activity in the presence of the novel object (Fig. 6 *C* and *D*). Post hoc analysis showed that wild-type mice exhibited greater horizontal and rearing activity than mutant mice. Heterozygous animals also displayed more rearing than mutant mice.

A substantial effect of genotype was also observed on the tail suspension test ($F_{2,20} = 26.49$, $P \leq 0.001$; Fig. 7). Post hoc analyses indicated that wild-type mice spent significantly more

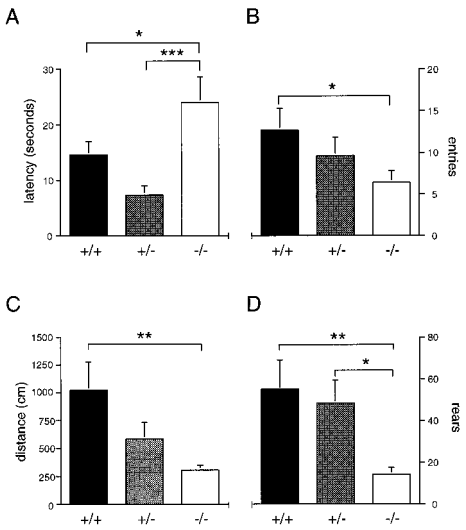

FIG. 6. Responses to a novel object. Mean (±SEM) (*A*) latency to approach a novel object placed in a familiar environment; (*B*) number of entries into area containing a novel object during a 30 min trial; (*C*) horizontal and (*D*) vertical activity during 30-min novel-object exposure. Significant differences by genotype are indicated as ***, $P \leq 0.001$; **, $P \leq 0.01$; *, $P \leq 0.05$.

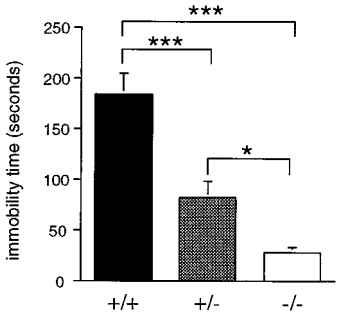

FIG. 7. Immobility in the tail-suspension assay. Mean (±SEM) time immobilized during the 6-min test. Significant differences by genotype are indicated as ***, $P \leq 0.001$; *, $P \leq 0.05$.

time immobile when suspended by the tail than did mutant and heterozygous animals, and that heterozygotes spent more time immobile than did homozygous mutant mice. Mutants displayed an 85% reduction in immobility relative to wild-type mice.

The above results were obtained in male mice. Female mice were separately assessed in the open-field, elevated-zero maze, and tail-suspension assays ($n = 10$ per genotype). Phenotype differences among females were less pronounced, but similar to males, with significantly elevated anxiety-like behavior in the open field and elevated-zero maze and reduced immobility in the tail-suspension assay in the mutants (data not shown).

To confirm the absence of 5-HT_{1A} receptor-mediated physiological responses in homozygous 5-HT_{1A} receptor mutant mice, thermoregulatory responses to 8-OH-DPAT were assessed. In mice, the hypothermic effects of this compound have been proposed to reflect its actions at somatodendritic 5-HT_{1A} autoreceptors (18). Because this effect peaked at 20 min posttreatment, changes in body temperature from baseline to this time were used for analysis. Repeated-measures ANOVA revealed a significant main effect of treatment ($F_{3,66} = 73.01$, $P \leq 0.001$) and genotype ($F_{2,22} = 29.32$, $P \leq 0.001$), and an interaction between treatment and genotype ($F_{6,66} = 13.24$, $P \leq 0.001$; Fig. 8). Post hoc comparisons indicated that the higher doses of 8-OH-DPAT (0.2, 1.0 mg/kg) were associated with hypothermia in wild-type and heterozygous animals. However, 5-HT_{1A} receptor mutant mice were insensitive to the hypothermic effects of 8-OH-DPAT at all doses administered.

DISCUSSION

We report the generation and behavioral analysis of a mouse strain bearing a targeted disruption of the serotonin 5-HT_{1A} receptor. The absence of functional 5-HT_{1A} receptors in these animals was confirmed by Northern blot analysis and receptor autoradiography and by the insensitivity of homozygous mutants to the hypothermic effect of 8-OH-DPAT. In accord with a substantial contribution of this receptor subtype to the serotonergic regulation of behavior, we find evidence for enhanced anxiety in the homozygous mutants and a marked antidepressant-like response in a rodent depression model. These behavioral phenotypes are not readily accounted for by perturbations of brain development. Examination of brain weights and Nissl-stained sections revealed no overt morphological abnormalities in 5-HT_{1A} receptor mutant mice. In addition, no abnormalities of serotonin system development were indicated by immunocytochemical analysis of serotonergic cell bodies and fibers or by determination of brain serotonin and 5-hydroxyindoleacetic acid (5-HIAA) content. These results are notable in light of the proposal that glial 5-HT_{1A} receptors influence brain development by stimulating the release of the neurotrophic factor S-100β, a protein that modulates the differentiation of neocortical and serotonergic neurons (19). These results do not exclude such a role for the 5-HT_{1A} receptor, as compensatory mechanisms may minimize the impact of its absence. In addition, the possibility that subtle developmental abnormalities exist cannot be excluded.

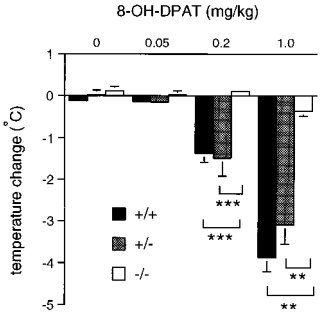

FIG. 8. Thermoregulatory responses to the administration of 8-OH-DPAT. Mean (±SEM) reduction in body temperature 20 min posttreatment (vehicle or 0.05, 0.2, 1.0 mg/kg 8-OH-DPAT; SC). Significant differences are indicated as ***, $P \leq 0.001$; **, $P \leq 0.01$.

Homozygous mutant mice displayed consistent elevations of anxiety-related behaviors in several assays that could not be accounted for by generalized phenotypic differences in locomotor activity. In the open field, mutants displayed a significant reduction in exploration of the central area, remaining in close proximity to the walls of the enclosure. The aversion to open spaces and seeking of cover, known as thigmotaxis, is a rodent behavior believed to correlate with anxiety (20, 21). Thigmotaxic responses were also assessed in the elevated-zero maze assay, a pharmacologically validated tool for the assessment of anxiety that measures aversion to an elevated open platform (22). Consistent with an increase in anxiety, mutants exhibited reduced time and activity in the open quadrants of the maze. In addition, they displayed fewer head dips, an exploratory behavior believed to inversely correlate with anxiety state (22). Moreover, mutants exhibited increased avoidance of a novel object, as indicated by elevated latencies to approach the object, diminished frequency of approach, and increased time spent in the nest area. Novel-object avoidance is believed to correlate with anxiety state (23). Thus, increased anxiety-like behaviors in response to an aversive environmental context generalized to a discrete novel object. Together, these findings suggest that 5-HT_{1A} receptor mutant mice exhibit elevated levels of anxiety.

Systemic administration of 5-HT_{1A} receptor agonists such as buspirone and antagonists such as WAY 100635 produce inconsistent effects on anxiety-related behaviors in various rodent models of anxiety (14, 24–27). This may relate to the existence of distinct 5-HT_{1A} receptor populations that produce opposing effects on anxiety regulation. For example, the stimulation of postsynaptic 5-HT_{1A} receptors of the dorsal hippocampus and amygdala has been proposed to elicit anxiogenic effects (28). In contrast, activation of 5-HT_{1A} autoreceptors is believed to produce anxiolytic effects via the suppression of serotonergic neuronal activity, with consequent decreased serotonin release in limbic terminal fields (6, 29–32). It is therefore possible that the enhancement of anxiety in 5-HT_{1A} receptor mutant mice reflects a disinhibition of serotonergic neuronal activity. Increased serotonin release in limbic terminal fields may enhance anxiety through the activation of other serotonin receptor subtypes. This possibility is not precluded by the normal tissue content of serotonin and 5-HIAA in the mutants, because the storage pools of serotonin vastly exceed extracellular serotonin content.

The modulation of serotonergic neural transmission is also proposed to be central to the therapeutic effects of antidepressant drugs, many of which increase the availability of serotonin at postsynaptic sites (33). It is therefore noteworthy that 5-HT_{1A} receptor mutant mice exhibited an 85% reduction

in immobility in the tail-suspension test, an assay used to evaluate the potential antidepressant efficacy of drugs. Antidepressants, including selective serotonin reuptake inhibitors, reduce the immobility displayed by mice following unsuccessful attempts to escape when suspended by the tail (34–36). The reduction in immobility time exhibited by 5-HT_{1A} receptor mutants is therefore indicative of a substantial antidepressant-like response.

5-HT_{1A} receptor activity is believed to influence the antidepressant effects of selective serotonin reuptake inhibitors such as fluoxetine. In the short term, the administration of such agents reduces serotonergic neuronal activity caused by the stimulation of 5-HT_{1A} autoreceptors. With chronic administration, however, these receptors are believed to gradually desensitize, leading to recovery of serotonergic neuronal activity; a phenomenon proposed to underlie the delayed onset of antidepressant action with these compounds (37). In accord with these phenomena, open-label studies have been conducted in which coadministration of 5-HT_{1A} receptor antagonists appears to accelerate the antidepressant effects of selective serotonin reuptake inhibitors (38). We therefore propose that the antidepressant-like responses of 5-HT_{1A} receptor mutants reflect a disinhibiton of serotonergic neuronal activity resulting from the absence of 5-HT_{1A} autoreceptors. Alternative explanations involving compensatory alterations of other neurotransmitter systems remain a possibility.

5-HT_{1A} receptor mutant mice provide a useful model for exploring the functional roles of this receptor subtype. Electrophysiological and microdialysis studies of these animals will aid in determining the extent to which their behavioral profile reflects enhanced serotonergic system activity. Evaluation of the neural mechanisms underlying the behavioral phenotypes of 5-HT_{1A} receptor mutant mice will shed light on the neural pathways relevant to the serotonergic regulation of anxiety and depression and on the actions of psychiatric drugs for these disorders.

We thank L. Guh, J. Schwenker, and R. Schroeder for technical assistance; R. Pedersen and J. Meneses for JM1 ES cells; and R. J. Rodgers, D. Nelson, C. Wichems, and L. Mamounas for helpful discussions. This work was supported by grants from the National Alliance for Research on Schizophrenia and Depression and the Giannini Foundation to L.K.H.; the National Alliance for Research on Schizophrenia and Depression to T.B.; Veterans Administration, National Alliance for Research on Schizophrenia and Depression and Program for Minority Research Training in Psychiatry to H.-M.C.; and the National Institute on Drug Abuse and the EJLB Foundation to L.H.T.

1. Bloom, F. E. & Kupfer, D. J. (1995) *Psychopharmacology: The Fourth Generation of Progress* (Raven, New York).
2. Hoyer, D., Clarke, D. E., Fozard, J. R., Hartig, P. R., Martin, G. R., Mylecharane, E. J., Saxena, P. R. & Humphrey, P. P. (1994) *Pharmacol. Rev.* **46,** 157–203.
3. Barrett, J. E. & Vanover, K. E. (1993) *Psychopharmacology* **112,** 1–12.
4. Artigas, F., Romero, L., de Montigny, C. & Blier, P. (1996) *Trends Neurosci.* **19,** 378–383.
5. Sotelo, C., Cholley, B., El Mestikawy, S., Gozlan, H. & Hamon, M. (1990) *Eur. J. Neurosci.* **2,** 1144–1154.
6. Sprouse, J. S. & Aghajanian, G. K. (1987) *Synapse* **1,** 3–9.
7. Pompeiano, M., Palacios, J. & Mengod, G. (1992) *J. Neurosci.* **12,** 440–453.
8. Fletcher, A., Bill, D. J., Cliffe, I. A., Forster, E. A. & Reilly, Y. (1994) *Br. J. Pharmacol.* **112,** 91P.
9. Dourish, C. T., Hutson, P. H. & Curzon, G. (1985) *Psychopharmacology* **86,** 197–204.
10. Hjorth, S. (1985) *J. Neural Transm.* **61,** 131–135.
11. Fletcher, A., Cliffe, I. A. & Dourish, C. T. (1993) *Trends Pharmacol. Sci.* **14,** 441–448.
12. File, S. E., Gonzalez, L. E. & Andrews, N. (1996) *J. Neurosci.* **16,** 4810–4815.
13. Forster, E. A., Cliffe, I. A., Bill, D. J., Dover, G. M., Jones, D., Reilly, Y. & Fletcher, A. (1995) *Eur. J. Pharmacol.* **281,** 81–88.
14. Fletcher, A., Forster, E. A., Bill, D. J., Brown, G., Cliffe, I. A., Hartley, J. E., Jones, D. E., McLenachan, A., Stanhope, K. J., Critchley, D. J., *et al.*(1996) *Behav. Brain Res.* 337–353.
15. Qiu, M., Bulfone, A., Martinez, S., Meneses, J. J., Shimamura, K., Pedersen, R. A. & Rubenstein, J. L. (1995) *Genes Dev.* **9,** 2523–2538.
16. Mansour, S. L., Thomas, K. R. & Capecchi, M. R. (1988) *Nature (London)* **336,** 348–352.
17. Chomczynski, P. & Sacchi, N. (1987) *Anal. Biochem.* **162,** 156–159.
18. Goodwin, G. M., De Souza, R. J. & Green, A. R. (1985) *Neuropharmacology* **24,** 1187–1194.
19. Whitaker-Azmitia, P. (1991) *Pharmacol. Rev.* **43,** 553–561.
20. Treit, D. & Fundytus, M. (1988) *Pharmacol. Biochem. Behav.* **31,** 958–962.
21. Simon, P., Dupuis, R. & Costentin, J. (1994) *Behav. Brain Res.* **61,** 59–64.
22. Shepherd, J. K., Grewal, S. S., Fletcher, A., Bill, D. J. & Dourish, C. T. (1994) *Psychopharmacology* **116,** 56–64.
23. Belzung, C. & Le Pape, G. (1993) *Physiol. Behav.* **56,** 623–628.
24. Cole, J. C. & Rodgers, R. J. (1994) *Psychopharmacology* **114,** 288–296.
25. Remy, S. M., Schreiber, R., Dalmus, M. & De Vry, J. (1996) *Psychopharmacology* **125,** 89–91.
26. Stanhope, K. J. & Dourish, C. T. (1996) *Psychopharmacology* **128,** 293–303.
27. Cao, B. J. & Rodgers, R. J. (1997) *Pharmacol. Biochem. Behav.* **58,** 593–603.
28. File, S. E. (1996) *Pharmacol. Biochem. Behav.* **54,** 3–12.
29. Higgins, G. A., Bradbury, A. J., Jones, B. J. & Oakley, N. R. (1988) *Neuropharmacology* **27,** 993–1001.
30. Sharp, F. R., Sagar, S. M. & Swanson, R. A. (1993) *Crit. Rev. Neurobiol.* **7,** 205–228.
31. Andrews, N., Hogg, S., Gonzales, L. E. & File, S. E. (1994) *Eur. J. Pharmacol.* **264,** 259–264.
32. De Vry, J. (1995) *Psychopharmacology* **121,** 1–26.
33. Blier, P. & de Montigny, C. (1994) *Trends Pharmacol. Sci.* **15,** 220–226.
34. Steru, L., Chermat, R., Thierry, B. & Simon, P. (1985) *Psychopharmacology* **85,** 367–370.
35. Steru, L., Chermat, R., Thierry, B., Mico, J. A., Lenegre, A., Steru, M. & Simon, P. (1987) *Prog. Neuropsychopharmacol. Biol. Psychiatry* **11,** 659–671.
36. van der Heyden, J. A., Molewijk, E. & Olivier, B. (1987) *Psychopharmacology* **92,** 127–130.
37. Blier, P., de Montigny, C. & Chaput, Y. (1987) *J. Clin. Psychopharmacol.* **7,** 24S–35S.
38. Blier, P. & Bergeron, R. (1998) *J. Clin. Psychiatry* **59,** Suppl. 5, 16–23; discussion 24–25.
39. Franklin, K. J. & Paxinos, G. (1997) *The Mouse Brain in Stereotaxic Coordinates* (Academic, San Diego).